

# Adaptive Reversible Watermarking Based on Linear Prediction for Medical Videos

Hamidreza Zarrabi, Ali Emami, Nader Karimi, Shadrokh Samavi

Department of Electrical and Computer Engineering,  
Isfahan University of Technology,  
Isfahan, 84156-83111 Iran

**Abstract**— Reversible video watermarking can guarantee that the original watermark and the original frame can be recovered from the watermarked frame without any distortion. Although reversible video watermarking has successfully been applied in multimedia, but its application has not been extensively explored in medical videos. Reversible watermarking in medical videos is still a challenging problem. The existing reversible video watermarking algorithms, which are based on error prediction expansion, use motion vectors for prediction. In this study, we propose an adaptive reversible watermarking method for medical videos. We suggest to use temporal correlations for improving the prediction accuracy. Hence, two temporal neighbor pixels in upcoming frames are used alongside the four spatial rhombus neighboring pixels to minimize the prediction error. To the best of our knowledge, this is the first time this method is applied for medical videos. The method helps to protect patients' personal and medical information by watermarking, i.e. increase the security of Health Information Systems (HIS). Experimental results demonstrate a high quality watermarking based on PSNR metric and a large capacity for data hiding on medical videos.

**Keywords**— component; Reversible Watermarking; Medical video; lossless Data Hiding

## I. INTRODUCTION

Thanks to constant development of computer technology, digital video acquisition is becoming much more convenient than ever for both online and offline applications [1]. Diagnostic and prognostic medical videos are vastly used by physicians for monitoring patients' tissues, internal organs and monitoring treatment procedures of patients. The recorded medical videos/images and patients' information are used by physicians for diagnosis. Medical videos are also used in medical research. The recorded medical videos/images and the patients' information are transmitted on public networks, such as internet and local computer networks. Therefore handling, sharing and processing of medical videos can lead to confidentiality, security and integrity issues [2,3]. These critical issues demand further research to ensure security of the medical videos and to provide solutions for content authentication.

Video watermarking is one of the solutions for aforementioned problems. Watermarking in medical videos could alter the media due to the embedded content. This distortion is not desired in medical applications. Even small distortions in a medical video may have impact on the

prognostic decision of the physician. One proposed solution is the use of reversible watermarking, such that both the original video and the watermark data can be restored from the watermarked video. Restoring of original medical videos ensures correct diagnostic and treatment. Therefore, reversible video watermarking is inevitable in health information system (HIS) which has attracted a lot of attention in the research community [1,4].

In reversible watermarking of medical videos, sensitive information, such as patient's ID, tag, diagnostic details, and signature, could be embedded into the video. This could be done by changing the pixels gray scale values without any perceptible changes on the host video. In other words, main idea of reversible video watermarking is to represent the original video, such that a new space for insertion of extra information is obtained in the proposed representation. By doing this, both the original medical video and the watermark can be fully restored [5].

Many reversible image watermarking methods exist in the literature. In [3], block based reversible watermarking is presented. Embedding is done in integer wavelet transform (IWT) coefficient and genetic programming as learning capability is exploited for intelligent selection of IWT coefficients. There is a tradeoff between capacity of watermark and imperceptibility. Histogram processing is used to avoid overflow/underflow problem. In [6], initial region of interest and non-region of interest is automatically extracted with adaptive threshold detector algorithm. Embedding is separately implemented for each region.

A very popular method for reversible image watermarking is based on Prediction Error Expansion (PEE) [7]. When overflow/underflow happens, the pixels is left unchanged and embedding is performed on the one of upper diagonal neighbors with different prediction errors.

In spite of many works on reversible watermarking, few researches can be found on reversible video watermarking [5]. A video signal is composed of consecutive frames. One possible solution for reversible video watermarking is to watermark single frames with reversible watermarking algorithms developed for images. However, this solution is not efficient, since temporal correlation between neighboring frames is not utilized. Reversible video watermarking methods with acceptable performance try to exploit interframe correlation. Fast motion video have low temporal correlation,

then watermarking with acceptable performance is another challenge.

In [5], motion compensated interpolation error is used for reversible video watermarking. Unlike other methods that use motion vectors, [5] applies interpolation error for increasing information capacity. Capacity of each frame is adaptively specified, so distortion distribution is equalized among frames.

In [8], a new robust reversible watermarking method for H.264/AVC video is proposed. In the beginning watermark is encoded using Bose–Chaudhuri–Hocquenghem syndrome code to increase robustness to attacks. Then information is embedded into quantized Discrete Cosine Transform (DCT) coefficients of 4×4 blocks of intra-coded frames. In [1], a new reversible watermarking method for H.264/AVC compressed video is proposed. It is shown that using histogram shifting of motion vectors could increase capacity.

In [9], reversible watermarking based on prediction in mosaic videos is proposed. To adaptively decrease prediction error, either Spatial or temporal correlation is exploited.

In [10], depth information is embedded into H.264 compressed video by quantized DCT coefficients expansion algorithm. A new efficient method is proposed for updating the entropy coding table.

The PEE method is shown to provide a better performance compared to other methods [11], i.e. higher capacity and lower distortion. In PEE method, lower prediction error is equivalent to lower distortion and higher embedding capacity. Exploiting both temporal and spatial correlation in videos, can help reduce prediction error, i.e. decrease distortion and increase the capacity [5,7].

Statistics of the image change from a region to another. Consequently, adaptive predictors can perform better than fixed predictors such as Median Edge Predictor (MEP), Gradient Adjusted Predictor (GAP), etc. [11].

In this paper, we propose an adaptive linear predictor for reversible watermarking in medical videos. The experimental results from three medical video sequences demonstrate that our proposed method performs well in terms of distortion and capacity. In this study, PEE method is used for reversible watermarking of medical videos. The proposed prediction scheme is linear and adaptive. Prediction coefficients are obtained by least square error method. In order to consider both temporal and spatial correlation, pixel  $x_{i,j}$  in frame  $k$  is predicted based on rhombus neighbors in  $k^{\text{th}}$  frame and its corresponding pixels in frames  $(k + 1)$  and  $(k + 2)$ .

The rest of this paper is organized as follows. The proposed method is discussed in section 2. Performance of the proposed method is investigated in section 3. Finally, contribution of our paper is summarized in section 4.

## II. PROPOSED METHOD

In part *A* of this section, we review PEE basics. Then in part *B*, we describe the proposed method.

### A. Overview of PEE Algorithms

In this section, we briefly explain PEE reversible image watermarking and linear prediction methods based on [7]. In embedding stage, given the pixel  $x_{i,j}$  and its prediction  $\hat{x}_{i,j}$ , the prediction error is calculated by

$$e_{i,j} = x_{i,j} - \hat{x}_{i,j} \quad (1)$$

Let's take a threshold  $t$  for realizing the capacity. If absolute prediction error is less than  $t$  and no overflow/underflow occurs, then new value of pixel is calculated by (2) and a bit of watermark,  $b$ , is embedded:

$$x'_{i,j} = x_{i,j} + e_{i,j} + b \quad (2)$$

If prediction error is greater than or equal to  $t$ , the pixel cannot be used for embedding. If there is no overflow/underflow, the pixel is modified by (3). This shift is necessary to provide greater prediction error compared to embedded pixels in the extraction stage, in order to guarantee reversibility.

$$x'_{i,j} = \begin{cases} x_{i,j} + t & \text{if } e_{i,j} \geq t \\ x_{i,j} - (t - 1) & \text{if } e_{i,j} \leq -t \end{cases} \quad (3)$$

In case of overflow/underflow, the pixels are left unchanged. Consequently, it is crucial for the extraction stage to differentiate between changed and unchanged pixels. If there are few unchanged pixels, one possible solution is to keep list of their coordinates. If the number of overflow/underflow pixels is large, we may provide a map of overflow/underflow pixels (e.g. 0 for unchanged pixels and 1 for changed pixels). The coordinate list or pixels map is embedded into the frame in raw/compressed form for extraction stage.

Let's suppose then, the extraction calculations must proceed the reverse order. In other words, the first extracted pixel should be the last embedded one. In extraction stage, given the pixel  $x'_{i,j}$  and its prediction  $\hat{x}_{i,j}$ , prediction error is calculated by

$$e'_{i,j} = x'_{i,j} - \hat{x}_{i,j} \quad (4)$$

Embedded pixels and shifted pixels are differentiated by prediction error. If the condition  $(-2t + 2 \leq e'_{i,j} \leq 2t - 1)$  is satisfied, an embedded pixel is reported, if no overflow/underflow occurs. Otherwise, the pixel is a shifted pixel, in case of no overflow/underflow. The original value of translated pixels is reconstructed by inverse of (3). For the embedded pixels, the original value is reconstructed by:

$$x_{i,j} = \frac{x'_{i,j} + \hat{x}_{i,j} - b}{2} \quad (5)$$

where the watermark bit  $b$ , is extracted from the LSB of  $e'_{i,j}$ .

In linear prediction, pixel  $x_{i,j}$  is predicted by a weighted sum of certain neighbor pixels via (6), as suggested in [11]:

$$\hat{x}_{i,j} = \text{floor}(\sum_{m=1}^n v_m x_{i,j}^m) \quad (6)$$

$x_{i,j}^1, \dots, x_{i,j}^n$  are the prediction contexts including the spatial and temporal neighbor pixels,  $n$  is the predictor order,  $m$  is index of prediction context and  $V = [v_1, \dots, v_n]^T$  is the column vector of predictor coefficients. One possible solution for finding predictor coefficients ( $V$ ) is the least square error method, as shown below:

$$V = (\mathbf{X}_{i,j}^T \mathbf{X}_{i,j})^{-1} \mathbf{X}_{i,j}^T \mathbf{y}_{i,j} \quad (7)$$

where  $\mathbf{X}_{i,j}$  is a matrix whose rows are the contexts vectors ( $[x_{i,j}^m]$ ) in (6) and  $\mathbf{y}_{i,j} = [x_{i,j}]^T$  is the context prediction vector.

For extraction, we want to calculate the prediction error. For this purpose, we need to know the original pixel value,  $x_{i,j}$ . However, the original value are not available in extraction stage. Consequently, we have to estimate the pixel value by averaging their context pixel. As long as the pixels have the same predicted value of equation (6), reversibility of watermarking is obtained. Therefore, before the calculation of  $\mathbf{X}_{i,j}$  and  $\mathbf{y}_{i,j}$ , pixel  $x_{i,j}$  is replaced by the estimated value.

## B. Proposed watermarking algorithm

### 1) Embedding procedure

A flowchart of the embedding procedure is presented in Fig.1. Inputs to the system are the video frames and the watermark image. Size of the watermark we use is constant in all frames. The system outputs are the watermarked video and a 23-bit string named 'S', which contains required extraction information. Coordinates of the final embedded pixel takes 19 bits of S and 3 bits are used to indicate the value of the threshold and 1 bit is for the checkerboard set, as explained in the next section.

We exploit the spatial correlation of neighbor pixels, in order to reduce the prediction error. The algorithm works on the diagonal pixels of a checkerboard pattern, as shown in Fig. 2. Hence, pixels on the checkerboard pattern, are divided into two distinct sets, cross (black) and dot (white). Embedding starts from the dot set pixels, until all of them are used up. The cross pixels will be used after processing all the dot pixels, in case further unembedded information exists. With this approach, we avoid using the previous embedded pixels for prediction as much as possible. The embedding process continues until all the watermark bits are embedded. Row, column and set of last embedded pixels are stored in the string 'S'.

We also exploit temporal correlation by using the pixels in the next two neighbor frames, in order to reduce the prediction

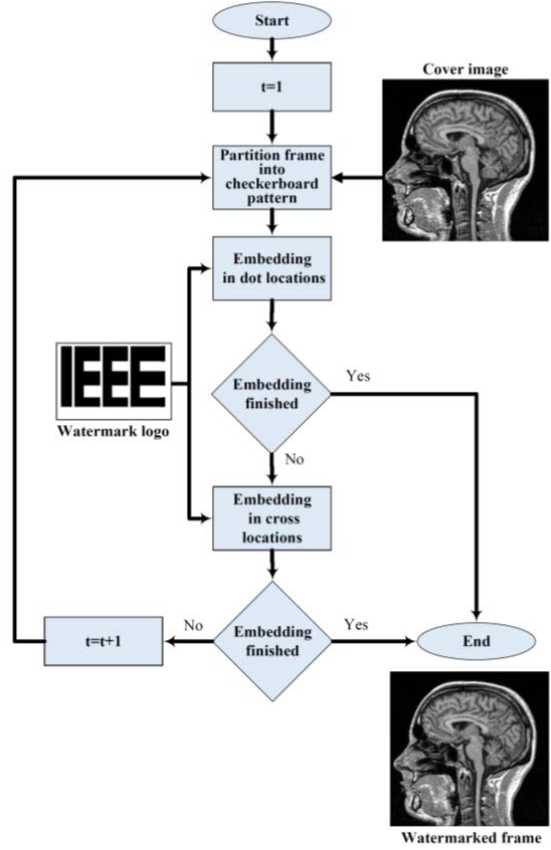


Figure 1. Flowchart of embedding procedure.

error. Hence, used frames for embedding are the unprocessed frames. The only exceptions are the last two frames in which their previous frames are used for prediction.

If any unembedded watermark bits remain after processing all pixels from both sets, we need to increase the threshold value for increasing the data capacity and start the whole process again. In the beginning, threshold  $t$  is set to '1' and then increased by 1, if further capacity is required. This makes the system adaptive to the required capacity. Parameter  $t$  is stored in the string 'S'.

Overflow/underflow pixels are left unchanged in the proposed method. We use a flag bit 'f' to differentiate between changed and unchanged pixels. These flag bits are embedded into the frame.

In least square error method, according to predictor order  $n$ , number of border pixels cannot be watermarked. In our method, border pixels in two-pixel thickness, cannot be embedded.

As mentioned before, in least square method, original value of pixels  $x_{i,j}$  cannot be used for their own prediction. Instead, we have to estimate a value for pixel. For this purpose, we use a simple rhombus predictor for estimating the pixel  $x_{i,j}$  is

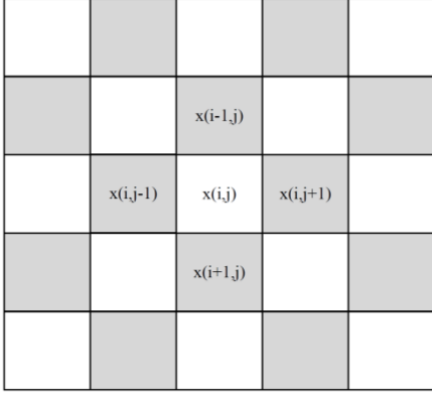


Figure 3. The checkerboard pattern used for embedding order of pixels.

predicted by fixed rhombus predictor (8). Since we want consider temporal correlation, its corresponding pixel in next frame are considered in (8). Let superscripts be frame number.

$$\hat{p}_{i,j} = \text{round}\left(\frac{x_{i-1,j}^k + x_{i+1,j}^k + x_{i,j-1}^k + x_{i,j+1}^k + x_{i,j}^{k+1}}{5}\right) \quad (8)$$

For each pixel  $x_{i,j}$ , the embedding algorithm is:

- $\hat{p}_{i,j}$  is calculated by (8) and  $X_{i,j}, y_{i,j}$  are created.
- Predictor coefficients ( $V$ ) are calculated by (7).
- The prediction of pixel  $x_{i,j}$  ( $\hat{x}_{i,j}$ ) is calculated by (6).
- Prediction error ( $e_{i,j}$ ) is calculated by (1).
- If  $t < |e_{i,j}|$ , then  $x'_{i,j}$  is calculated by (2) (embedding), otherwise calculated by (3) (shifting).
- If  $x'_{i,j} \in [0,255]$  (no overflow/underflow):
  - $x_{i,j}$  is replaced by  $x'_{i,j}$ .
  - If  $(x'_{i,j} \leq (t-2) \text{ or } x'_{i,j} \geq (256-t))$ , then flag bit  $f=1$  is inserted into the next embeddable pixel.
- If  $x'_{i,j} \notin [0,255]$  (overflow/underflow), then do not replace  $x_{i,j}$  and insert flag bit  $f=0$  into the next embeddable pixel.

## 2) Extraction procedure

Flowchart of the extraction procedure is presented in Fig. 3. Inputs are watermarked video frames and the string 'S'. Outputs are reconstructed video frames and the watermark image.

For each pixel  $x'_{i,j}$ , the extraction algorithm is:

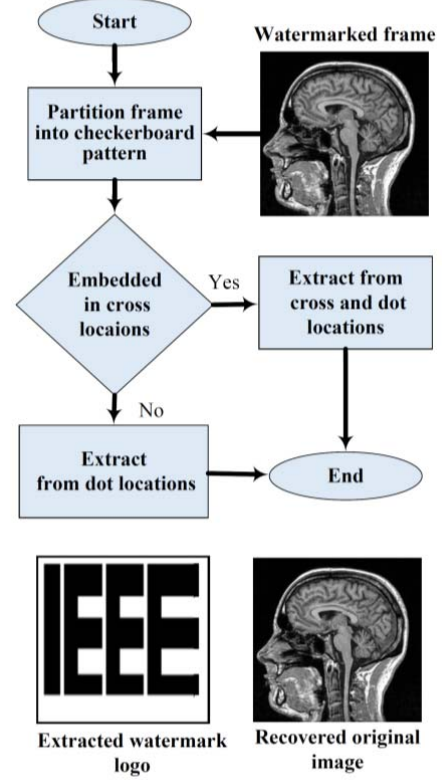


Figure 2. Flowchart of Extraction procedure.

- $\hat{p}_{i,j}$  is calculated by (8) and  $X_{i,j}, y_{i,j}$  are created.
- Predictor coefficients ( $V$ ) are calculated by (7).
- The prediction of pixel  $x'_{i,j}$  ( $\hat{x}_{i,j}$ ) is calculated by (6).
- Prediction error ( $e'_{i,j}$ ) is calculated by (4).
- If  $(-2t + 2 \leq e'_{i,j} \leq 2t - 1)$ 
  - If  $(x'_{i,j} \leq (t-2) \text{ or } x'_{i,j} \geq (256-t))$  and its corresponding flag bit is '1', an embedded pixel is reported. The watermark bit,  $b$ , is extracted from the LSB of  $e'_{i,j}$  and the original value is reconstructed by (5).
  - If  $(x'_{i,j} \leq (t-2) \text{ or } x'_{i,j} \geq (256-t))$  and its corresponding flag bit is '0', an unchanged pixel is reported.
  - If condition  $(t-2 < x'_{i,j} < 256-t)$  is satisfied, an embedded pixel is reported. The watermark bit,  $b$ , is extracted from the LSB of  $e'_{i,j}$  and the original value is reconstructed by (5).

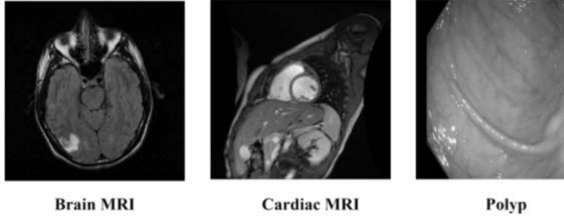


Figure 4. Frames of three test medical videos.

- If  $(e'_{i,j} > (2t - 1) \text{ or } (-2t + 2) > e'_{i,j})$ 
  - If  $(x'_{i,j} \leq (t - 2) \text{ or } x'_{i,j} \geq (256 - t))$  and its corresponding flag bit is '1', a shifted pixel is reported. Then, original value is reconstructed by inverting (3).
  - If  $(x'_{i,j} \leq (t - 2) \text{ or } x'_{i,j} \geq (256 - t))$  and its corresponding flag bit is '0', an unchanged pixel is reported.
  - If condition  $(t - 2 < x'_{i,j} < 256 - t)$  is satisfied, a shifted pixel is reported. Then, original value is reconstructed by inverting (3).

### III. RESULTS

Performance of the described reversible watermarking algorithm is tested on three medical video sequences (Brain MRI [12], Cardiac MRI [13] and Polyp [14]). Test videos demonstrate different motion rates. The Cardiac MRI sequence has moderate motion, the Brain MRI sequence has fast motion and Polyp sequence has slow motion. Sample frames of the three datasets are shown in Fig. 4 for visual demonstration. Each sequence includes 18 frames. The frame size of Brain MRI and Cardiac MRI sequences is  $256 \times 256$ , but Polyp frames have a bigger size of  $480 \times 856$ . For the input watermark, we use a binary image with an equal distribution of ones and zeros (48% ones and 52% zeros).

In Fig. 5 original frame and watermarked frame for each sequence is shown. It can be seen that watermarked frame is visually identical to original frame. For evaluating the performance of our algorithm, we calculate the capacity and distortion of the watermarked frames. Watermarking capacity in each frame is calculated by the ratio of total number of watermark bits to the total number of pixels in the frame, expressed in bit per pixel (BPP):

$$BPP = \frac{L}{W \times H} \quad (9)$$

where  $L$  is the total number of watermark bits,  $W$  and  $H$  are the frame's width and height respectively.

For evaluating the distortion of frames, we have used Peak Signal to Noise Ratio (PSNR) [3] as a metric, which is described in (10):

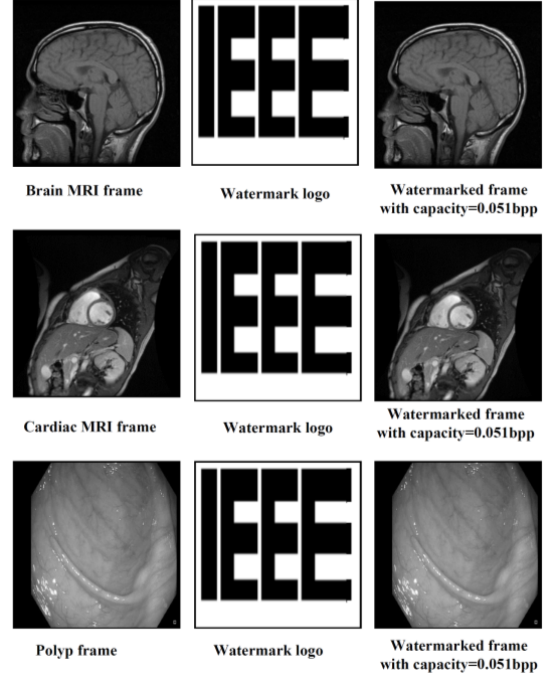


Figure 5. Original frames, watermark logo, and watermarked frames.

$$PSNR = 10 \log_{10} \frac{255^2}{\frac{1}{N \times W \times H} \sum_{k=1}^N \sum_{i,j=1}^{W,H} (F_{i,j}^w(k) - F_{i,j}(k))^2} \quad (10)$$

where  $N$  is count of frames,  $W$  and  $H$  are width and height of frames respectively.  $F_{i,j}(k)$  and  $F_{i,j}^w(k)$  are pixel  $(i, j)$  in frame  $k$  of original and watermarked videos respectively.

Table 1 summarizes the capacity-distortion results of our proposed method for the three medical sequences. We divide the video sequence into 3 groups, where each group of frames contain 6 frames. Table I indicates that distortions in different groups of one sequence are almost equal and even near to that

TABLE I. AVERAGE PSNR FOR DIFFERENT CAPACITIES.

Watermark size		32×32	45×45	52×65
Average PSNR of Brain MRI video (dB)	Group 1	58.8585	54.6089	52.6738
	Group 2	59.9209	54.9546	53.1324
	Group 3	58.5134	54.5059	52.286
	All groups	59.187	54.6817	52.6942
Average PSNR of Cardiac MRI Video (dB)	Group 1	63.6774	60.4947	58.3929
	Group 2	63.4404	60.3482	58.3454
	Group 3	63.4382	60.3423	58.3062
	All groups	63.5875	60.4381	58.3764
Average PSNR of Polyp video (dB)	Group 1	74.1876	71.0835	68.7212
	Group 2	74.0803	71.1009	68.7336
	Group 3	74.8347	71.6936	69.3134
	All groups	74.5175	71.4508	69.0291

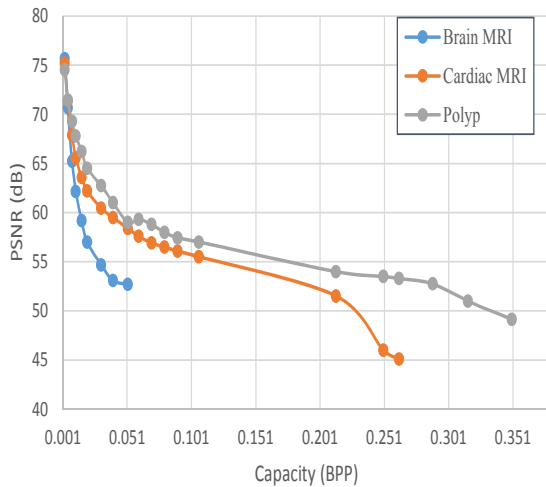


Figure 6. PSNR as a function of capacity for the proposed method.

of the whole sequence which is the union of the groups in that sequence. These results also demonstrate that the proposed method is almost independent of the number of the frames of sequence. As we can see watermark image of size  $52 \times 65$  is successfully embedded into the fast motion MRI sequence. When embedding the small watermark of size  $32 \times 32$  in Polyp sequence, results in PSNR=74dB, implying a very low distortion. It is shown that increasing the watermark size to almost double, doesn't lead to proportional increase of distortion, i.e. for the watermark size of  $52 \times 65$ . The proposed method provides an acceptable low distortion on all of the three medical sequences of our experiments.

Fig. 6 shows distortion-capacity results of the three experiments. Three observations may be noticed in these plots. Firstly, increasing the watermark size, does not lead to proportional increase in distortion. Secondly, the faster is the motion, a lower capacity is available for reversible watermarking. For the fast motion Brain MRI, maximum capacity is 0.051 BPP, while the slow Polyp sequence provides a maximum capacity of 0.351 BPP. Thirdly, the faster is the motion, we observe a higher distortion. The Cardiac MRI curve, demonstrate PSNR of 46dB for a capacity of 0.251 BPP, while the Polyp curve shows PSNR of 54dB for the same embedding capacity.

#### IV. CONCLUSION

In this paper, we have investigated a new method for reversible watermarking in medical videos. This means that original videos can be reconstructed from the watermarked frames. Unlike previous methods, which embedding and extraction of watermarks are based on motion vectors, we apply a linear adaptive predictor. To increase the watermark capacity, temporal correlation has been exploited for prediction. We have shown that watermark image of size  $52 \times 65$  can be embedded in the fast motion Brain MRI with a very low distortion (PSNR=52dB). The proposed method is also applicable for non-medical videos.

#### REFERENCES

- [1] K. Niu, X. Yang, and Y. Zhang, "A Novel Video Reversible Data Hiding Algorithm Using Motion Vector for H.264/AVC," vol. 22, no. 5, 2017.
- [2] M. Arsalan, A. S. Qureshi, A. Khan, and M. Rajarajan, "Protection of medical images and patient related information in healthcare: Using an intelligent and reversible watermarking technique," *Appl. Soft Comput. J.*, vol. 51, pp. 168–179, 2017.
- [3] C. Vural and B. Baraklı, "Reversible video watermarking using motion-compensated frame interpolation error expansion," *Signal, Image Video Process.*, vol. 9, no. 7, pp. 1613–1623, 2015.
- [4] M. P. Turuk and A. P. Dhande, "A Novel Reversible Multiple Medical Image Watermarking for Health Information System," *J. Med. Syst.*, vol. 40, no. 12, 2016.
- [5] C. Vural and İ. Yıldırım, "Reversible video watermarking through recursive histogram modification," *Multimed. Tools Appl.*, vol. 76, no. 14, pp. 15513–15534, 2017.
- [6] Y. Yang, W. Zhang, D. Liang, and N. Yu, "A ROI-based high capacity reversible data hiding scheme with contrast enhancement for medical images," *Multimed. Tools Appl.*, 2017.
- [7] I. Dragoi, "Towards Overflow / Underflow Free PEE Reversible Watermarking," pp. 953–957, 2016.
- [8] Y. Liu, L. Ju, M. Hu, X. Ma, and H. Zhao, "A robust reversible data hiding scheme for H.264 without distortion drift," *Neurocomputing*, vol. 151, no. P3, pp. 1053–1062, 2015.
- [9] K.-L. Chung, C.-Y. Chiu, T.-Y. Yu, and P.-L. Huang, "Temporal and spatial correlation-based reversible data hiding for RGB CFA videos," *Inf. Sci. (Ny)*, vol. 420, pp. 386–402, 2017.
- [10] W. Wang and J. Zhao, "Hiding depth information in compressed 2D image/video using reversible watermarking," *Multimed. Tools Appl.*, vol. 75, no. 8, pp. 4285–4303, 2016.
- [11] I. Dragoi and D. Coltuc, "Local-Prediction-Based Difference Expansion," vol. 23, no. 4, pp. 1779–1790, 2014.
- [12] <http://overcode.yak.net>
- [13] <https://www.cse.yorku.ca/~mridataset/>
- [14] <https://polyp.grand-challenge.org/site/Polyp/AsuMayo/>